

**Supporting information**

**Three microporous metal-organic frameworks assembled from dodecanuclear  $\{\text{Ni}^{\text{II}}_6\text{Ln}^{\text{III}}_6\}$  subunits:**

**Synthesis, structure, gas adsorption and magnetism**

Dan-Dan Feng,<sup>a</sup> Hui-Ming Dong,<sup>a</sup> Zheng-Yu Liu,<sup>a</sup> Xiao-Jun Zhao<sup>\*a,b</sup> and En-Cui Yang<sup>\*a</sup>

<sup>a</sup> College of Chemistry, Key Laboratory of Inorganic-Organic Hybrid Functional Material Chemistry, Ministry of Education, Tianjin Key Laboratory of Structure and Performance for Functional Molecules, Tianjin Normal University, Tianjin 300387, People's Republic of China

<sup>b</sup> Department of Chemistry, Collaborative Innovation Center of Chemical Science and Engineering, Nankai University, Tianjin 300071, People's Republic of China

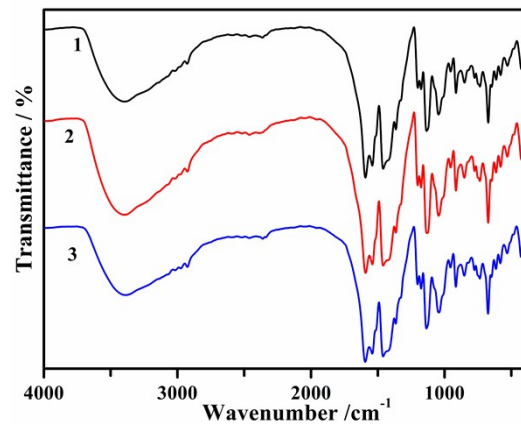


**Fig. S1** FT-IR spectra for **1–3**.

**Table S1** Agreement factors for the Ln<sup>III</sup> ions in **1–3** calculated by SHAPE program\*

Ideal polyhedron geometry	MFF ( $C_s$ )	CSAPR ( $C_{4v}$ )	JCSAPR ( $C_{4v}$ )	TCTPR ( $D_{3h}$ )
Agreement factor for Dy <sup>III</sup>	1.775	1.875	2.512	2.540
Agreement factor for Tb <sup>III</sup>	1.766	1.875	2.523	2.567
Agreement factor for Gd <sup>III</sup>	1.690	1.781	2.422	2.625

\*MFF = Muffin, CSAPR = Spherical capped square antiprism, JCSAPR = Capped square antiprism, TCTPR = Spherical tricapped trigonal prism.

**Table S2** Selected Bond Lengths ( $\text{\AA}$ ) and Angles (deg) for **1**<sup>a</sup>

Dy(1)–O(1)	2.3833(15)	Dy(1)–O(7)	2.3042(16)
Dy(1)–O(3)	2.4436(15)	Dy(1)–N(1)	2.5493(18)
Dy(1)–O(4) <sup>#1</sup>	2.3193(15)	Dy(1)–N(3)	2.4923(18)
Dy(1)–O(4)	2.5509(15)	Ni(1)–O(1)	2.1138(15)
Dy(1)–O(5)	2.4357(17)	Ni(1)–N(2) <sup>#2</sup>	2.1281(18)
Dy(1)–O(6)	2.4241(17)	Ni(1)–N(5)	2.0218(19)
O(1)–Dy(1)–O(3)	85.35(5)	O(6)–Dy(1)–N(3)	72.89(6)
O(1)–Dy(1)–O(4)	76.25(5)	O(7)–Dy(1)–O(1)	148.77(5)
O(1)–Dy(1)–O(5)	130.12(6)	O(7)–Dy(1)–O(3)	80.86(6)
O(1)–Dy(1)–O(6)	77.75(5)	O(7)–Dy(1)–O(4)	73.16(5)
O(1)–Dy(1)–N(1)	125.90(5)	O(7)–Dy(1)–O(4) <sup>#1</sup>	83.69(5)
O(1)–Dy(1)–N(3)	63.56(5)	O(7)–Dy(1)–O(5)	73.93(6)
O(3)–Dy(1)–O(4)	52.02(5)	O(7)–Dy(1)–O(6)	127.25(6)
O(3)–Dy(1)–N(1)	69.19(6)	O(7)–Dy(1)–N(1)	74.50(6)
O(3)–Dy(1)–N(3)	72.38(5)	O(7)–Dy(1)–N(3)	135.82(6)
O(4) <sup>#1</sup> –Dy(1)–O(1)	80.09(5)	N(1)–Dy(1)–O(4)	115.79(5)
O(4) <sup>#1</sup> –Dy(1)–O(3)	121.95(5)	N(3)–Dy(1)–O(4)	112.85(5)
O(4) <sup>#1</sup> –Dy(1)–O(4)	69.94(6)	N(3)–Dy(1)–N(1)	63.46(6)
O(4) <sup>#1</sup> –Dy(1)–O(5)	84.43(6)	O(1) <sup>#1</sup> –Ni(1)–O(1)	110.56(8)
O(4) <sup>#1</sup> –Dy(1)–O(6)	85.00(6)	O(1)–Ni(1)–N(2) <sup>#2</sup>	87.00(6)
O(4) <sup>#1</sup> –Dy(1)–N(3)	140.38(6)	O(1) <sup>#1</sup> –Ni(1)–N(2) <sup>#3</sup>	87.00(6)
O(5)–Dy(1)–O(3)	141.16(6)	O(1)–Ni(1)–N(2) <sup>#3</sup>	87.64(6)
O(5)–Dy(1)–O(4)	139.97(6)	O(1) <sup>#1</sup> –Ni(1)–N(2) <sup>#2</sup>	87.63(6)
O(5)–Dy(1)–N(1)	75.80(6)	N(5)–Ni(1)–O(1)	77.81(7)
O(5)–Dy(1)–N(3)	106.55(6)	N(5) <sup>#1</sup> –Ni(1)–N(2) <sup>#2</sup>	94.50(7)
O(6)–Dy(1)–O(3)	145.22(5)	N(5)–Ni(1)–N(2) <sup>#3</sup>	94.50(7)
O(6)–Dy(1)–O(4)	146.43(6)	N(5)–Ni(1)–N(2) <sup>#2</sup>	91.94(7)
O(6)–Dy(1)–O(5)	53.75(6)	N(5) <sup>#1</sup> –Ni(1)–N(2) <sup>#3</sup>	91.94(7)
O(6)–Dy(1)–N(1)	96.63(6)	N(5) <sup>#1</sup> –Ni(1)–N(5)	93.85(11)

<sup>a</sup> Symmetry codes: <sup>#1</sup>  $x, 1 - y, 3/2 - z$ ; <sup>#2</sup>  $x, 3/2 - y, z - 1/2$ ; <sup>#3</sup>  $1 - x, y, z - 1/2$ .

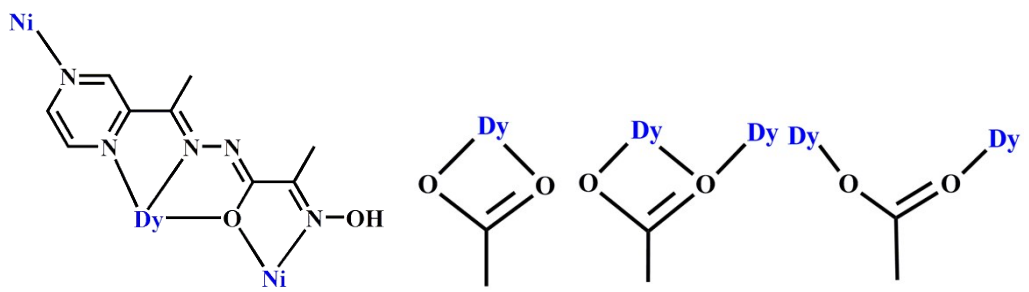


**Fig. S2** Binding mode of HL ligand and  $\text{OAc}^-$  anion observed in **1**.

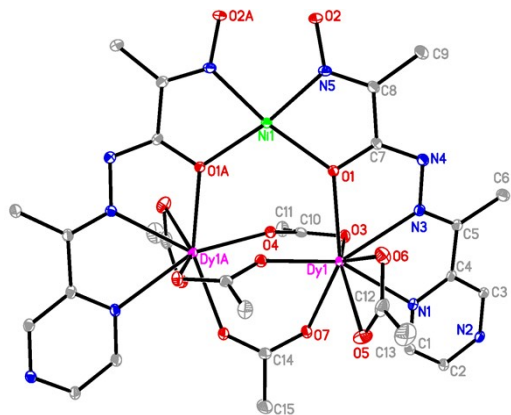


**Fig. S3** Ortep of the  $[\text{Dy}_2\text{Ni}(\text{OAc})_5(\text{HL})(\text{L})]$  unit (displacement ellipsoids were shown at the 30% probability level, H atoms were omitted for clarity, symmetry code  $\text{A} = x, 1 - y, 1.5 - z$ ).

**Table S3** Selected Bond Lengths ( $\text{\AA}$ ) and Angles (deg) for **2**<sup>a</sup>

Tb(1)–O(1)	2.3921(18)	Tb(1)–O(7)	2.318(2)
Tb(1)–O(3)	2.4540(19)	Tb(1)–N(1)	2.562(2)
Tb(1)–O(4)	2.5600(18)	Tb(1)–N(3)	2.501(2)
Tb(1)–O(4) <sup>#1</sup>	2.3282(18)	Ni(1)–O(1)	2.1153(18)
Tb(1)–O(5)	2.427(2)	Ni(1)–N(2) <sup>#2</sup>	2.133(2)
Tb(1)–O(6)	2.443(2)	Ni(1)–N(5)	2.022(2)
O(1)–Tb(1)–O(3)	85.13(6)	O(6)–Tb(1)–N(1)	96.56(8)
O(1)–Tb(1)–O(4)	76.37(6)	O(6)–Tb(1)–N(3)	72.87(7)
O(1)–Tb(1)–O(5)	130.01(9)	O(7)–Tb(1)–O(1)	148.70(7)
O(1)–Tb(1)–O(6)	77.68(8)	O(7)–Tb(1)–O(3)	80.82(8)
O(1)–Tb(1)–N(1)	125.68(7)	O(7)–Tb(1)–O(4)	72.95(7)
O(1)–Tb(1)–N(3)	63.58(6)	O(7)–Tb(1)–O(4) <sup>#1</sup>	83.80(7)
O(3)–Tb(1)–O(4)	51.69(6)	O(7)–Tb(1)–O(5)	74.35(10)
O(3)–Tb(1)–N(1)	69.51(7)	O(7)–Tb(1)–O(6)	127.43(9)
O(3)–Tb(1)–N(3)	72.50(6)	O(7)–Tb(1)–N(1)	74.71(7)
O(4) <sup>#1</sup> –Tb(1)–O(1)	80.14(6)	O(7)–Tb(1)–N(3)	135.74(7)
O(4) <sup>#1</sup> –Tb(1)–O(3)	121.89(6)	N(3)–Tb(1)–O(4)	112.91(6)
O(4) <sup>#1</sup> –Tb(1)–O(4)	70.20(7)	N(3)–Tb(1)–N(1)	63.20(7)
O(4) <sup>#1</sup> –Tb(1)–O(5)	84.70(8)	O(1)–Ni(1)–O(1) <sup>#1</sup>	110.86(10)
O(4) <sup>#1</sup> –Tb(1)–O(6)	84.77(7)	O(1) <sup>#1</sup> –Ni(1)–N(2) <sup>#2</sup>	87.88(8)
O(4)–Tb(1)–N(1)	115.78(7)	O(1) <sup>#1</sup> –Ni(1)–N(2) <sup>#3</sup>	87.12(8)
O(4) <sup>#1</sup> –Tb(1)–N(3)	140.36(7)	O(1)–Ni(1)–N(2) <sup>#2</sup>	87.12(8)
O(5)–Tb(1)–O(3)	141.30(8)	O(1)–Ni(1)–N(2) <sup>#3</sup>	87.88(8)
O(5)–Tb(1)–O(4)	140.41(8)	N(5)–Ni(1)–O(1)	77.64(8)
O(5)–Tb(1)–O(6)	53.57(10)	N(5) <sup>#1</sup> –Ni(1)–N(2) <sup>#2</sup>	94.24(9)
O(5)–Tb(1)–N(1)	75.52(8)	N(5)–Ni(1)–N(2) <sup>#2</sup>	91.77(9)
O(5)–Tb(1)–N(3)	106.00(8)	N(5) <sup>#1</sup> –Ni(1)–N(2) <sup>#3</sup>	91.77(9)
O(6)–Tb(1)–O(3)	145.31(7)	N(5)–Ni(1)–N(2) <sup>#3</sup>	94.24(9)
O(6)–Tb(1)–O(4)	146.48(8)	N(5) <sup>#1</sup> –Ni(1)–N(5)	93.88(13)

<sup>a</sup> Symmetry codes: <sup>#1</sup>  $x, 1 - y, 3/2 - z$ ; <sup>#2</sup>  $x, 3/2 - y, z - 1/2$ ; <sup>#3</sup>  $1 - x, y, z - 1/2$ .

**Table S4** Selected Bond Lengths ( $\text{\AA}$ ) and Angles (deg) for **3<sup>a</sup>**

Gd(1)–O(1)	2.402(4)	Gd(1)–O(7)	2.330(4)
Gd(1)–O(6)	2.474(5)	Gd(1)–N(1)	2.573(5)
Gd(1)–O(5)	2.426(5)	Gd(1)–N(3)	2.512(5)
Gd(1)–O(3)	2.345(4)	Ni(1)–O(1)	2.124(4)
Gd(1)–O(3) <sup>#1</sup>	2.562(4)	Ni(1)–N(2) <sup>#2</sup>	2.146(5)
Gd(1)–O(4) <sup>#1</sup>	2.469(4)	Ni(1)–N(5)	2.022(5)
O(1)–Gd(1)–O(6)	75.63(16)	O(4) <sup>#1</sup> –Gd(1)–N(1)	69.94(14)
O(1)–Gd(1)–O(5)	130.33(18)	O(4) <sup>#1</sup> –Gd(1)–N(3)	72.64(14)
O(1)–Gd(1)–O(3) <sup>#1</sup>	75.46(12)	O(7)–Gd(1)–O(1)	148.15(14)
O(1)–Gd(1)–O(4) <sup>#1</sup>	84.04(13)	O(7)–Gd(1)–O(6)	129.60(18)
O(1)–Gd(1)–N(1)	124.90(14)	O(7)–Gd(1)–O(5)	75.4(2)
O(1)–Gd(1)–N(3)	63.34(14)	O(7)–Gd(1)–O(3) <sup>#1</sup>	73.21(14)
O(6)–Gd(1)–O(3) <sup>#1</sup>	143.33(16)	O(7)–Gd(1)–O(3)	84.09(14)
O(6)–Gd(1)–N(1)	98.73(17)	O(7)–Gd(1)–O(4) <sup>#1</sup>	81.01(16)
O(6)–Gd(1)–N(3)	72.73(16)	O(7)–Gd(1)–N(1)	75.39(15)
O(5)–Gd(1)–O(6)	55.3(2)	O(7)–Gd(1)–N(3)	135.98(15)
O(5)–Gd(1)–O(3) <sup>#1</sup>	142.20(18)	N(3)–Gd(1)–O(3) <sup>#1</sup>	112.70(13)
O(5)–Gd(1)–O(4) <sup>#1</sup>	141.26(17)	N(3)–Gd(1)–N(1)	62.79(16)
O(5)–Gd(1)–N(1)	74.59(17)	O(1) <sup>#1</sup> –Ni(1)–O(1)	110.9(2)
O(5)–Gd(1)–N(3)	104.43(19)	O(1) <sup>#1</sup> –Ni(1)–N(2) <sup>#2</sup>	87.66(16)
O(3)–Gd(1)–O(1)	79.84(13)	O(1)–Ni(1)–N(2) <sup>#2</sup>	88.34(16)
O(3)–Gd(1)–O(6)	83.39(16)	O(1) <sup>#1</sup> –Ni(1)–N(2) <sup>#3</sup>	88.34(16)
O(3)–Gd(1)–O(5)	86.71(16)	O(1)–Ni(1)–N(2) <sup>#3</sup>	87.66(16)
O(3)–Gd(1)–O(3) <sup>#1</sup>	69.70(14)	N(5)–Ni(1)–O(1)	77.75(17)
O(3)–Gd(1)–O(4) <sup>#1</sup>	121.12(13)	N(5)–Ni(1)–N(2) <sup>#2</sup>	92.4(2)
O(3) <sup>#1</sup> –Gd(1)–N(1)	116.25(14)	N(5) <sup>#1</sup> –Ni(1)–N(2) <sup>#3</sup>	92.4(2)
O(3)–Gd(1)–N(3)	139.78(14)	N(5) <sup>#1</sup> –Ni(1)–N(2) <sup>#2</sup>	92.4(2)
O(4) <sup>#1</sup> –Gd(1)–O(6)	144.91(16)	N(5)–Ni(1)–N(2) <sup>#3</sup>	92.4(2)
O(4) <sup>#1</sup> –Gd(1)–O(3) <sup>#1</sup>	51.44(12)	N(5) <sup>#1</sup> –Ni(1)–N(5)	93.6(3)

<sup>a</sup> Symmetry codes: <sup>#1</sup>  $x, -y, 1/2 - z$ ; <sup>#2</sup>  $1/2 - x, 1/2 - y, 1/2 - z$ ; <sup>#3</sup>  $x, 1/2 - y, z - 1/2$ .

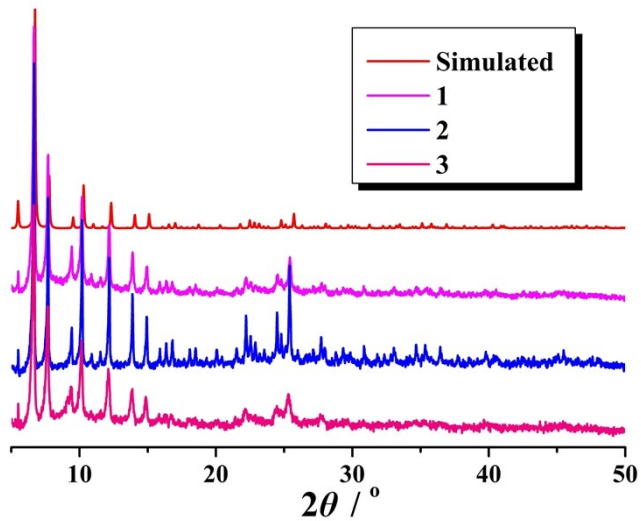


**Fig. S4** Simulated and experimental PXRD patterns for **1–3**.

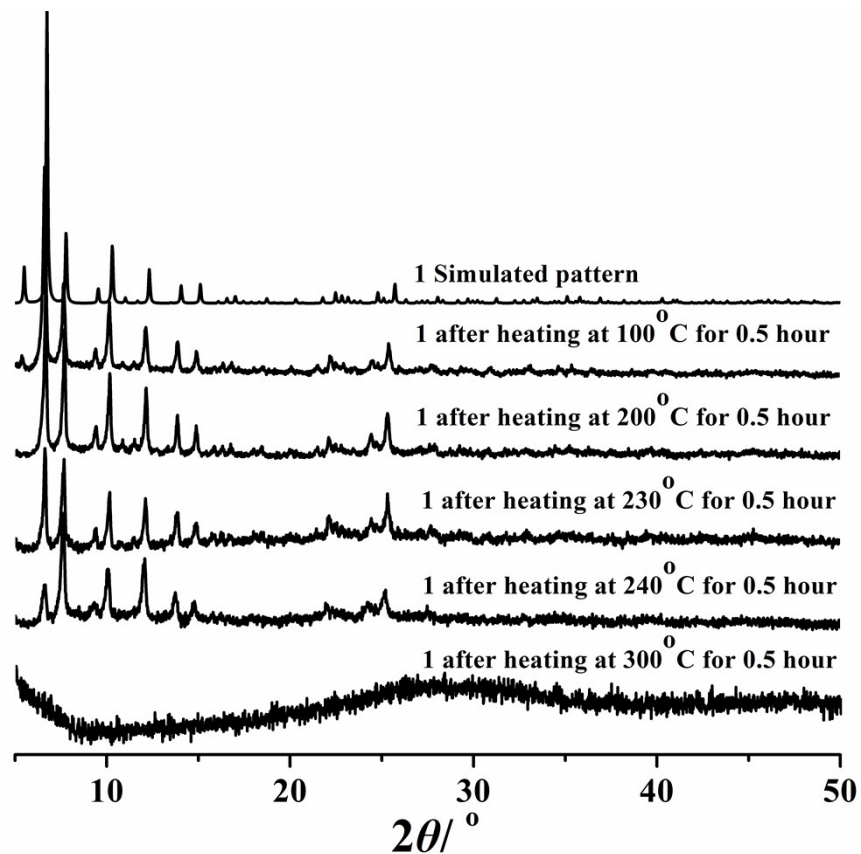


**Fig. S5** Simulated and experimental PXRD patterns of **1** after heating at different temperatures for half an hour.

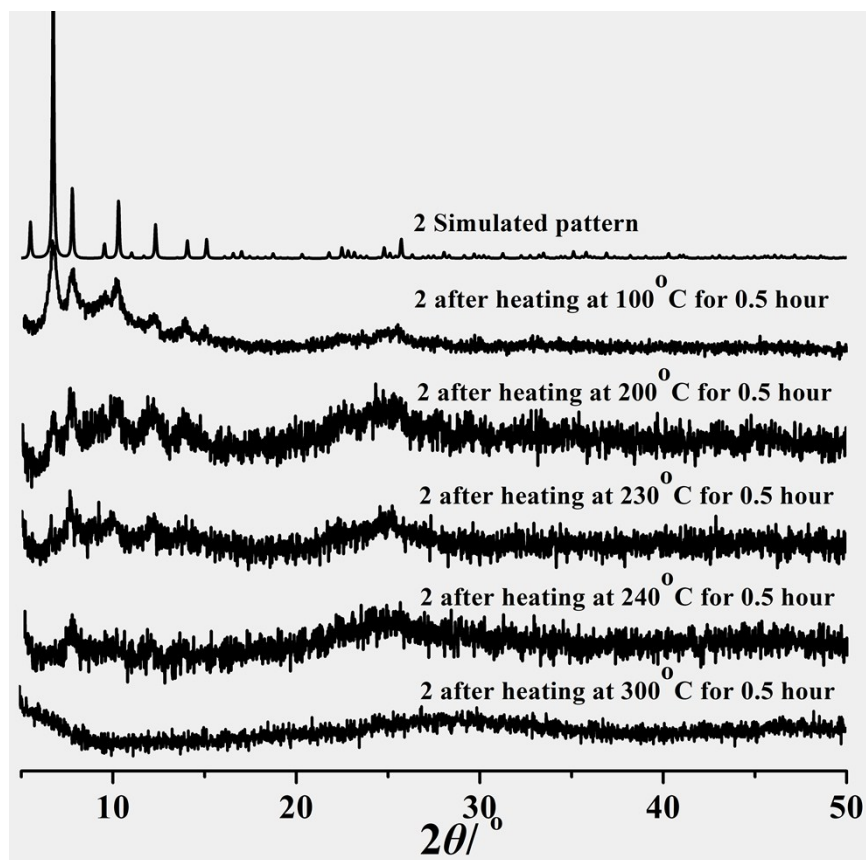


**Fig. S6** Simulated and experimental PXRD patterns of **2** after heating at different temperatures for half an hour.

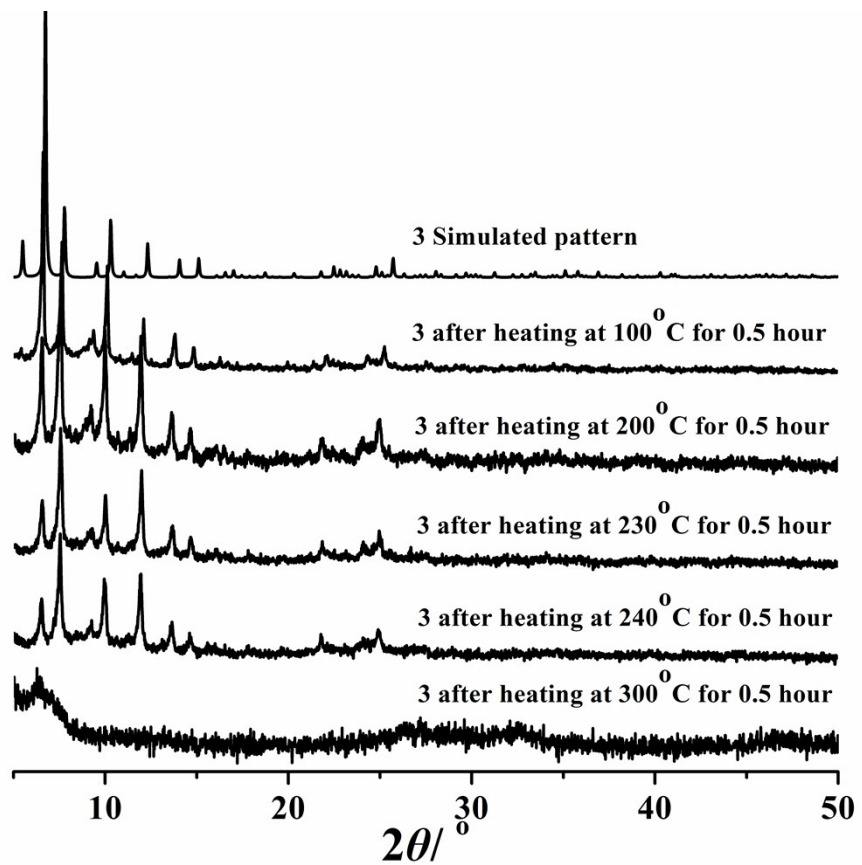


**Fig. S7** Simulated and experimental PXRD patterns of **3** after heating at different temperatures for half an hour.

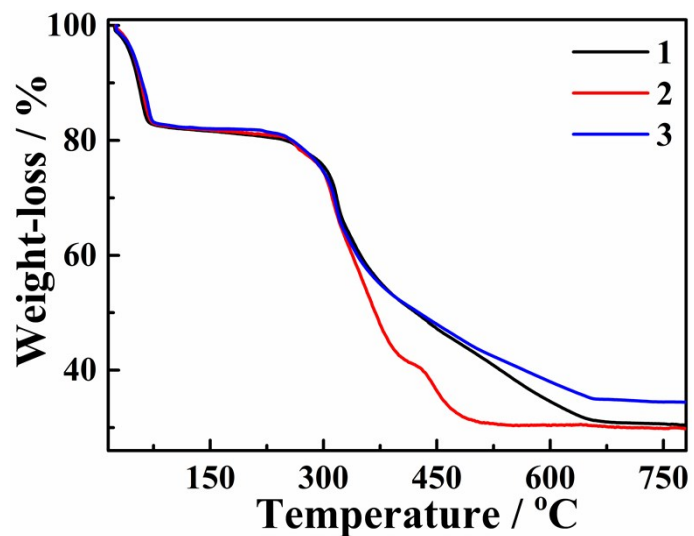
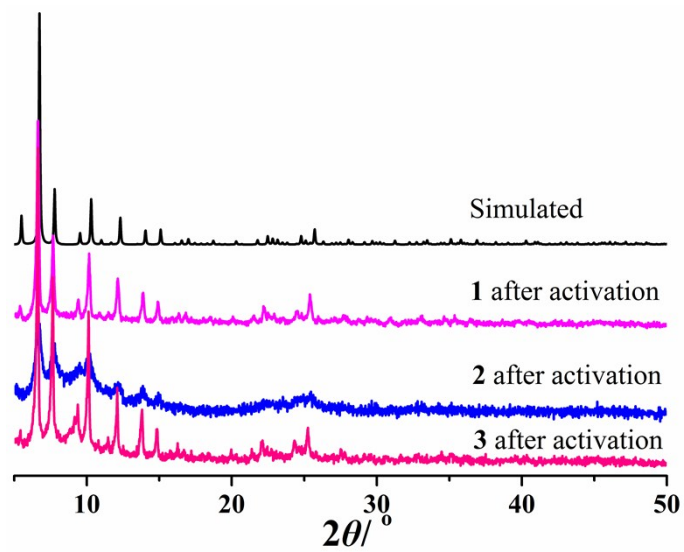
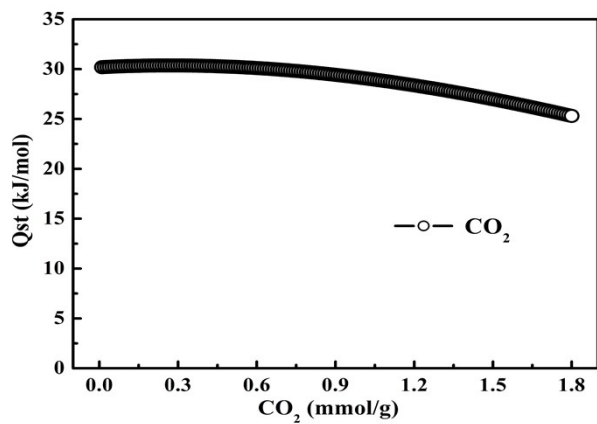


Fig. S8 TG curves for 1–3.



**Fig. S9** Simulated and experimental PXRD patterns of **1–3** after activation.



**Fig. S10** The adsorption enthalpy of CO<sub>2</sub>.

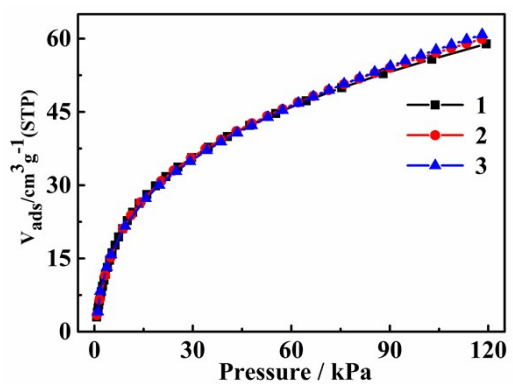


**Fig. S11** CO<sub>2</sub> adsorption isotherms for the activated samples of **1–3** at 273 K.

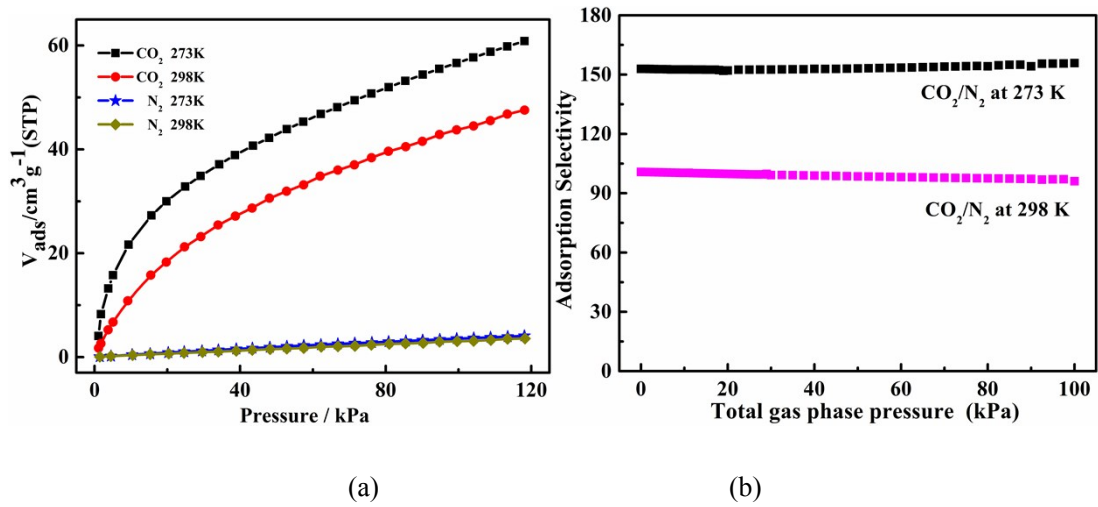


**Fig. S12.** (a)  $\text{CO}_2$  and  $\text{N}_2$  adsorption isotherms at 273 K and 298 K. (b) IAST calculated absorption selectivity from 15:85  $\text{CO}_2/\text{N}_2$  gas-phase mixtures at 273 K and 298 K based upon the experimentally observed adsorption isotherm of the pure gas.

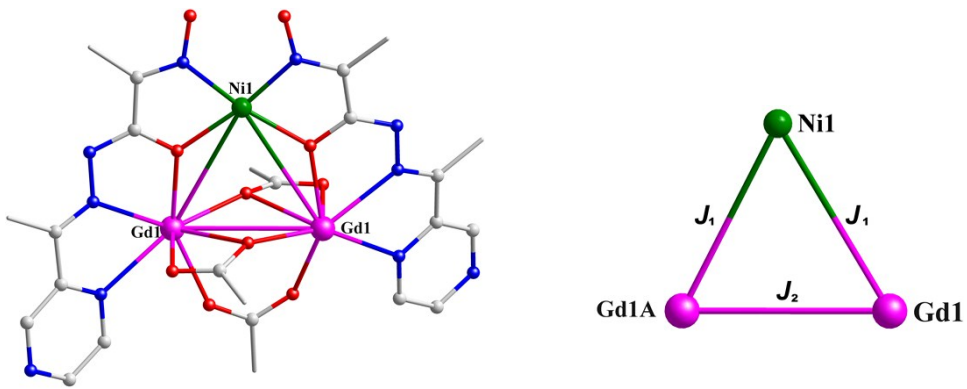


**Fig. S13** Magnetic pathways for complex **3**.

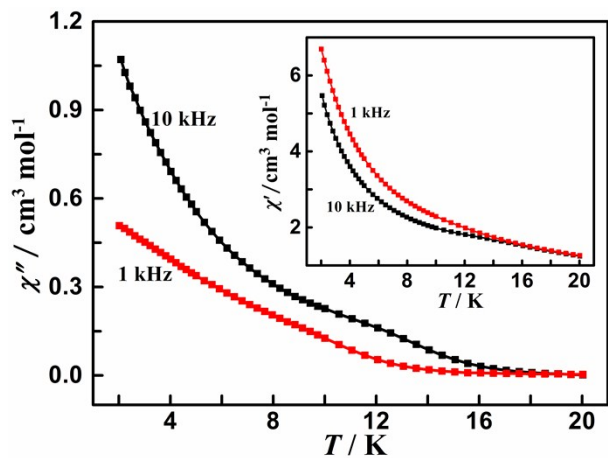


**Fig. S14** Temperature dependence of the in-phase and out-of-phase ac susceptibilities for **1** measured under  $H_{\text{dc}} = 2.0$  kOe and  $H_{\text{ac}} = 3.5$  Oe.

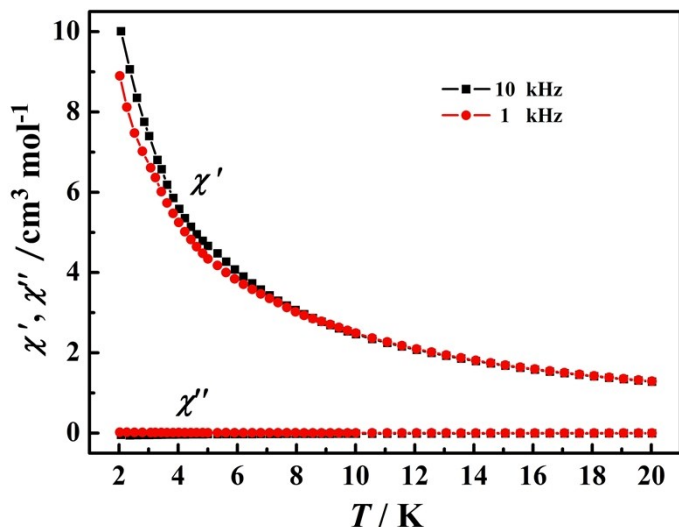


**Fig. S15** Temperature dependence of the in-phase and out-of-phase ac susceptibilities for **2** measured under  $H_{\text{dc}} = 0$  kOe and  $H_{\text{ac}} = 3.5$  Oe.